Research Square

Preprints are preliminary reports that have not undergone peer review.
They should not be considered conclusive, used to inform clinical practice,
or referenced by the media as validated information.

Integrated Network Pharmacology and Metabolomics Reveals the Multi-Target Mechanism of Ginsenosides in Anti-Fibrinolysis After Hip Arthroplasty

Xiaoyan Yao
Army Medical University
Yuanlin Du
Army Medical University
Sai Cao
Southwest University
Lei Tan
Southwest University
Yi Hu
Army Medical University
Qingxiang Mao
maomaosmmu@126.com
Army Medical University

Article

Keywords: Ginsenosides, Total hip arthroplasty, Fibrinolysis, Network pharmacology, Metabolomics, Molecular docking

Posted Date: June 24th, 2026

DOI: https://doi.org/10.21203/rs.3.rs-9609939/v1

License: This work is licensed under a Creative Commons Attribution 4.0 International License.
Read Full License

Additional Declarations: No competing interests reported.

Abstract

Introduction:

Total hip arthroplasty (THA) is an effective treatment for end-stage hip joint diseases but is frequently associated with postoperative hyperfibrinolysis, which elevates the risks of bleeding and thrombosis. Ginsenosides, the primary active components of Panax ginseng, exhibit a range of pharmacological activities, including anti-inflammatory and anti-apoptotic effects. However, their mechanism of action in counteracting postoperative hyperfibrinolysis after THA remains unclear.

Methods

Active ginsenoside components were first screened from databases such as TCMSP and BATMAN-TCM on the basis of ADME parameters. Key targets were identified through network pharmacology, followed by the construction of a protein–protein interaction (PPI) network and GO and KEGG enrichment analyses. Meanwhile, venous blood samples were collected from THA patients at 2 hours preoperatively and 24 hours postoperatively for untargeted metabolomics analysis using LC-MS/MS. Multivariate statistical analysis was applied to screen differential metabolites and perform pathway enrichment. Finally, the results of network pharmacology and metabolomics were integrated to construct a “component–target–metabolic pathway” association network.

Results

A total of 9 active ginsenoside components were obtained, yielding 351 component-related targets and 428 fibrinolysis-related targets, with an intersection of 65 key targets. PPI network analysis identified AKT1, PTGS2, and JUN as core targets. KEGG enrichment analysis revealed significant enrichment in the complement and coagulation cascades, platelet activation, and HIF-1 signaling pathways. Metabolomics identified 292 differential metabolites, mainly enriched in arachidonic acid metabolism, purine metabolism, and glycerophospholipid metabolism. Integrative analysis identified arachidonic acid metabolism and the cGMP-PKG, cAMP, and sphingolipid signaling pathways as common key pathways. Molecular docking of AKT1 with ginsenoside Rh7, JUN with ginsenoside Rg3, PIK3CA with ginsenoside Rh1, and PTGS2 with F2 all demonstrated favorable binding affinity, further supporting the reliability of the network pharmacology predictions.

Conclusion

This study is the first to systematically elucidate that ginsenosides modulate postoperative fibrinolysis following THA by regulating multiple targets (e.g., AKT1 and PTGS2) and multiple pathways (including

arachidonic acid metabolism and the complement and coagulation cascades), thereby providing a new theoretical basis for their perioperative clinical application.

Introduction

Total joint arthroplasty (TJA), including total hip arthroplasty (THA) and total knee arthroplasty (TKA), is the most effective surgical treatment for end-stage joint diseases. It significantly relieves pain, restores joint function, and corrects deformities [1]. With the aging population, the number of TJA procedures is projected to increase by 174%–673% by 2030 [2, 3], drawing increasing attention to perioperative management. However, as a major orthopedic surgery, TJA is often accompanied by a pronounced stress response and a dynamic imbalance in the coagulation–fibrinolysis system postoperatively [4]. Early postoperative hyperfibrinolysis is a key contributor to hidden blood loss, increased allogeneic transfusion rates, and prolonged hospital stays. It may also elevate the risk of venous thromboembolism (VTE) due to a rebound hypercoagulable state following fibrinolysis [5, 6]. Although anticoagulant prophylaxis is now widely used, the overall incidence of symptomatic VTE after THA remains approximately 1.3%, while the risk of major bleeding is at least 0.5%. This dual “thrombosis–bleeding” risk constitutes the core dilemma in fibrinolysis management [7]. Therefore, exploring safe and effective strategies to regulate the fibrinolytic balance after TJA is of significant clinical importance.

Ginsenosides, the primary active components of *Panax ginseng* C. A. Meyer, have been shown to possess a wide range of pharmacological activities, including anti-inflammatory, antioxidant, anti-apoptotic, and cardiovascular protective effects [8, 9]. In recent years, growing research has focused on their potential to regulate hematological functions. Studies have reported that ginsenosides can inhibit platelet aggregation and modulate the activity of coagulation factors [10, 11]. However, a systematic investigation into the effects of ginsenosides on the postoperative fibrinolytic system in the context of TJA-induced surgical stress, as well as the underlying molecular mechanisms, is still lacking.

Network pharmacology, a systems biology approach, can reveal the synergistic mechanisms of multi-component, multi-target traditional Chinese medicines from a holistic “drug–component–target–pathway” perspective. Li Xiao et al. demonstrated through network pharmacology that the combined use of *Bupleurum chinense* and *Paeonia lactiflora* significantly enhanced the antidepressant effect [12]. Li Teng et al. found that hydroxysafflor yellow A (HSYA) exerts significant therapeutic effects on traumatic brain injury (TBI) by acting on multiple targets, including NOS1, ACHE, PTGS2, and XDH [13]. These findings highlight the crucial role of multi-target synergy in the therapeutic actions of traditional Chinese medicine. On the other hand, metabolomics, by detecting dynamic changes in small-molecule metabolites in vivo, can sensitively capture the functional phenotypic alterations following disease states or drug interventions. Hui et al. showed through metabolomics that parthenolide alleviates methamphetamine-induced depression by regulating the ADORA2A signaling pathway in the medial prefrontal cortex (mPFC) [14], further underscoring the power of metabolomics in elucidating drug mechanisms.

This study proposes the hypothesis that ginsenosides may exert antifibrinolytic effects after TJA by acting on multiple targets and regulating several fibrinolysis-related metabolic pathways. To test this hypothesis, we will integrate network pharmacology with untargeted metabolomics analysis of clinical samples. First, network pharmacology will be used to predict the potential targets and pathways of ginsenosides in antifibrinolysis. Then, metabolomics will be employed to identify differential metabolites in postoperative serum samples from TJA patients, which will subsequently be integrated with the network pharmacology predictions. Finally, a “component–target–metabolic pathway” network will be constructed through integrative analysis, and molecular docking will be applied to validate the core targets. This study aims to systematically elucidate the molecular mechanisms by which ginsenosides regulate postoperative fibrinolysis in TJA, providing a scientific basis for their rational clinical application.

Materials and Methods

Screening of Active Ginsenoside Components and Target Prediction

Using "Ginsenoside" as the keyword, the Traditional Chinese Medicine Systems Pharmacology Database and Analysis Platform (TCMSP, https://tcmsp-e.com/) and the BATMAN-TCM database (http://bionet.ncpsb.org.cn/batman-tcm/) were searched. Screening conditions based on pharmacokinetic parameters were set: Oral Bioavailability (OB) ≥ 20% and Drug-Likeness (DL) ≥ 0.1 [15]. Relevant literature [16] was also consulted to ensure the inclusion of components with well-defined biological activity, even if ADME parameters were slightly lower. This process yielded the candidate active ginsenoside components.

The Canonical SMILES structural formulas or 2D structures of the screened active components were imported into the SwissTargetPrediction (http://www.swisstargetprediction.ch/) and PharmMapper(http://www.lilab-ecust.cn/pharmmapper/) databases, with the species limited to "Homo sapiens," to predict their potential targets. The results from both databases were integrated, duplicates were removed, and the set of potential targets for the active ginsenoside components was obtained.

Collection of Fibrinolysis-Related Targets

Using "fibrinolysis" as the keyword, the GeneCards (https://www.genecards.org/) and Online Mendelian Inheritance in Man (OMIM, https://omim.org/) databases were searched. For the GeneCards database, targets with a Relevance score ≥ 10 were selected as high-confidence fibrinolysis-related targets. The results from both databases were integrated and duplicates removed to obtain the set of fibrinolysis-related targets.

Network Construction and Core Target Screening

The ginsenoside target set and the fibrinolysis-related target set were intersected to obtain potential targets for the anti-fibrinolytic effect of ginsenosides. The intersection targets were submitted to the STRING database (https://string-db.org/), with the species set to "Homo sapiens" and a minimum required interaction score of 0.4 (medium confidence), to construct a protein-protein interaction (PPI) network. The PPI network data were imported into Cytoscape 3.9.1 software for visualization. Using the CytoHubba plugin, the top 20 targets based on Maximal Clique Centrality (MCC) algorithm were selected as core targets (Hub genes).

Gene Function Enrichment Analysis

To investigate the biological functions of the core targets, the intersection targets were imported into the DAVID database (https://david.ncifcrf.gov/) or Metascape database (https://metascape.org/) for Gene Ontology (GO) functional enrichment analysis and Kyoto Encyclopedia of Genes and Genomes (KEGG) pathway enrichment analysis. A significance threshold of $P < 0.05$ was used to identify significantly enriched terms and pathways.

Clinical Sample Collection and Metabolomics Analysis

Ethics

The ethical approval for this study (IRB No: 2021 – 168) was provided by the Ethics Committee of Daping Hospital, Army Medical University, on October 20, 2021 (Jingjing Wang approved the protocol). All methods were performed in accordance with the relevant guidelines and regulations. Confirm that informed consent has been obtained from all participants and/or their legal guardians. This study was conducted in accordance with the Helsinki Declaration. The datasets used and/or analyzed during the current study are available from the corresponding author on reasonable request. The study protocol was registered with the Chinese Clinical Trial Registry on January 8, 2022 (Registration No: ChiCTR2200055399).

Study Participants and Sample Collection

This study was approved by the ethics committee, and all patients provided informed consent. A total of 30 patients undergoing elective unilateral TJA between January 2022 and June 2022 were enrolled. We included a total of 30 patients in the study. As shown in the figures, 30 elderly patients aged 65 to 89 years who underwent elective arthroplasty surgery (including total hip arthroplasty and total knee arthroplasty) were selected, regardless of sex and nationality. The American Society of Anesthesiologists (ASA) system was used to determine whether patients had grade II or III disease, and patients had no mental or nervous system disease before surgery. Individuals who fulfilled any of the exclusion criteria listed below were excluded: (1) had a history of cognitive dysfunction or surgery that affected cognitive function or drug use that affected cognitive function; (2) had hyperlipidemia, diabetes

mellitus, or other metabolic diseases; (3) had neurological disorders, including stroke, schizophrenia, epilepsy, or Parkinson's disease; (4) participated in other clinical trials within the last 3 months; (5) had a history of hearing loss or speech-language disorders; (6) were dependent on alcohol or drugs; (7) had severe bradycardia or sick sinus syndrome; and (8) refused to participate in the study. Peripheral venous blood (5 mL) was collected from these patients 2 hours preoperatively (T0) and 24 hours postoperatively (T1) into EDTA anticoagulant tubes. After resting for 30 minutes, the samples were centrifuged at 3000 rpm for 15 minutes at 4°C. The separated upper plasma layer was aliquoted and stored at -80°C for later use.

Ultra-High Performance Liquid Chromatography Tandem Q Exactive Mass Spectrometry Analysis

LC-MS/MS analysis was performed using an ultra-high performance liquid chromatography system (Vanquish, Thermo Fisher Scientific) equipped with a UPLC BEH amide column (2.1 mm × 100 mm, 1.7 μm) coupled to a Q Exactive HFX mass spectrometer (Orbitrap MS, Thermo). The mobile phase consisted of water (containing 25 mmol/L ammonium acetate and 25 mmol/L ammonium hydroxide, pH = 9.75) (A) and acetonitrile (B). The autosampler temperature was set to 4°C, and the injection volume was 2 μL. Raw data were converted to mzXML format using ProteoWizard software. Peak identification, extraction, alignment, and integration were performed using a self-developed R package (based on XCMS). Detected mass spectrometry information was matched against substance annotation algorithms in a self-built BiotreeDB secondary mass spectrometry database. BiotreeDB is a database integrating information from public databases such as HMDB, MONA, and METLIN, containing information on over 20,000 substances from these sources. The data included m/z, fragmentation spectra, retention time, HMDB ID, CAS number, INCHIKEY, and classification information. Substances meeting the criteria of VIP > 1 and P < 0.05 were considered significantly differential metabolites. Detection and analysis were completed by Shanghai Biotree Biomedical Technology Co., Ltd.

Data Preprocessing and Statistical Analysis

Raw data were preprocessed using Compound Discoverer 3.0 software for peak alignment, peak extraction, and deconvolution. The data were imported into SIMCA-P 14.1 software for Principal Component Analysis (PCA) and Orthogonal Partial Least Squares Discriminant Analysis (OPLS-DA). Differential metabolites between the preoperative (T0) and postoperative (T1) time points were screened based on a Variable Importance in Projection (VIP) > 1 from the OPLS-DA model and a P-value < 0.05 from independent sample t-tests. Differential metabolites were identified by comparison with databases such as HMDB, KEGG, and mzCloud. The differential metabolites were imported into MetaboAnalyst 5.0 for metabolic pathway enrichment analysis, using a Pathway Impact > 0.1 as the criterion for identifying significant pathways.

Integration of Network Pharmacology and Metabolomics

Significant metabolic pathways identified from metabolomics analysis were intersected with significant pathways identified from KEGG enrichment in network pharmacology to identify "common pathways." Based on these common pathways, a multi-dimensional association network of "ginsenoside components-core targets- differential metabolites-common pathways" was constructed. Visualization was performed using Cytoscape software and its MetScape plugin.

Molecular Docking Validation

To validate the binding ability of core components with core targets, selected core targets from the PPI network with high Degree values (AKT1, PTGS2, JUN, PIK3CA) were subjected to molecular docking with active ginsenoside components (Rh7, Rh1, Rg3, F2). 3D structures (SDF format) of active components were downloaded from the PubChem database (https://pubchem.ncbi.nlm.nih.gov/) and converted to mol2 format using OpenBabel software. Crystal structures of target proteins were downloaded from the PDB database (http://www.rcsb.org/). Preprocessing, including adding hydrogens and calculating charges, was performed using AutoDock Tools. Semi-flexible docking was performed using AutoDock Vina. A binding energy < -5 kcal/mol was generally considered indicative of good binding activity. Docking results were visualized using PyMol. We have presented the methods outlined in Fig. 1.

Statistical Analysis

All data were statistically analyzed using SPSS 25.0 software. Measurement data are presented as mean ± standard deviation. Comparisons between two groups were performed using independent sample t-tests. A P-value < 0.05 was considered statistically significant.

Results

Results of Network Pharmacology Analysis

Based on ADME parameter screening, a total of nine active ginsenoside components meeting the criteria were identified, including ginsenosides Rh7, Rh2, Rh1, Rg5, Rg3, Rg2, F3, F2, and R2. Through target prediction databases, 351 ginsenoside-related targets were obtained. After searching and deduplicating the GeneCards and OMIM databases, 428 fibrinolysis-related targets were identified. Mapping the 351 ginsenoside targets onto the 428 fibrinolysis targets yielded 65 intersecting targets, which were considered potential key targets for ginsenosides in regulating fibrinolysis (Fig. 2A, Table 1). These 65 intersecting targets were imported into STRING to construct a protein-protein interaction (PPI) network, which comprised 65 nodes and 426 edges (Fig. 2B). Using the CytoHubba plugin in Cytoscape, the top 20 targets based on the MCC algorithm were selected as core targets (Fig. 2C). Among these, targets with high Degree values, such as AKT1, PTGS2, JUN, VEGFA, PIK3CA, SRC, and MMP9, were considered potentially central to the anti-fibrinolytic effect of ginsenosides.

KEGG pathway enrichment analysis showed that the 20 potential targets were significantly enriched in pathways such as “Complement and coagulation cascades,” “Platelet activation,” “HIF-1 signaling

pathway," and "VEGF signaling pathway" (Fig. 2D). GO enrichment analysis indicated that biological processes (BP) were mainly enriched in "phosphatidylinositol-mediated signaling," "blood coagulation," and "regulation of inflammatory response"; cellular components (CC) mainly involved "plasma membrane" and "platelet alpha granule lumen"; and molecular functions (MF) mainly involved "protein kinase activity" and "enzyme binding" (Fig. 2E). Based on the above data analysis, we constructed a "component–target–pathway–disease" network (Fig. 2F).

Results of Metabolomics Analysis

The PCA score plot showed tight clustering of QC samples, indicating good system stability and reliable data quality (Fig. 3A). Permutation testing (200 times) showed that the Q^2 and R^2 values were lower than the original point, suggesting that the established model was valid and effective (Fig. 3B). In the OPLS-DA score plot, samples from the preoperative (Pre) and 24 h postoperative (Pos) time points showed significant separation, indicating substantial changes in the plasma metabolic profile of patients after TJA (Fig. 3C). The S-plot from OPLS-DA revealed various metabolites (Fig. 3D). Volcano plot analysis identified 306 differential metabolites between the preoperative and postoperative time points; compared with the preoperative state, 143 metabolites were significantly upregulated, and 163 were significantly downregulated (Fig. 3E). Using the criteria of VIP > 1 and $P < 0.05$, a total of 292 differential metabolites were screened (Fig. 3F). These 292 differential metabolites were imported into MetaboAnalyst for pathway enrichment analysis. The results showed that the significant metabolic pathways after TJA mainly included arachidonic acid metabolism, purine metabolism, and glycerophospholipid metabolism (Fig. 3G–H).

Integration of Network Pharmacology and Metabolomics

Intersecting the pathways enriched from the KEGG analysis of ginsenoside targets on fibrinolysis with the pathways enriched from metabolomics identified a total of 13 common pathways (Fig. 4A). Among these 13 pathways, arachidonic acid metabolism, the cGMP-PKG signaling pathway, the cAMP signaling pathway, and the sphingolipid signaling pathway were considered the most critical, as they contained both core targets and differential metabolites (Fig. 4B). Metabolite–gene–disease association and metabolite–gene association analyses revealed key metabolites and key genes (Fig. 4C–D). By matching the potential targets identified in network pharmacology with genes from the MetScape analysis, we identified four key targets, including AKT1, PTGS2, PIK3CA, and JUN (Fig. 4E–G). Ginsenosides may regulate core targets such as AKT1, PTGS2, and PIK3CA, subsequently affecting key metabolites like arachidonic acid, prostaglandins, and adenosine, ultimately achieving coordinated regulation of multiple pathways, including the complement and coagulation cascades, platelet activation, and arachidonic acid metabolism.

Analysis of Key Pathways

To comprehensively understand the anti-fibrinolytic mechanism of ginsenosides, an interaction network was constructed based on metabolomics and network pharmacology. The pathways most relevant to fibrinolysis were listed, including the cAMP/cGMP signaling pathway, arachidonic acid metabolism, and the sphingolipid signaling pathway (Fig. 5A–D).

Molecular Docking Validation

Molecular docking was performed between the core target AKT1 and ginsenoside Rh7, JUN and ginsenoside Rg3, PIK3CA and ginsenoside Rh1, as well as PTGS2 and F2. The results showed that the binding energies for all docking combinations were less than − 5.0 kcal/mol, indicating strong binding affinity between the active components and target proteins (Table 2). Among them, the binding energy between ginsenoside Rh7 and AKT1 was − 5.1 kcal/mol, with tight hydrogen bonding to amino acid residues such as GLU-405 and TRP-414. The binding energy between ginsenoside Rh1 and PIK3CA was the lowest (–9.59 kcal/mol) (Fig. 6). The active pockets of F2 and PTGS2 also formed stable hydrogen bonding interactions. These findings further validated the reliability of the network pharmacology predictions.

Discussion

Joint arthroplasty profoundly affects the body's fibrinolytic balance by activating both the coagulation and fibrinolysis systems. Studies have shown that patients undergoing total hip arthroplasty (THA) already exhibit preoperative fibrinolytic dysfunction. Specifically, levels of tissue plasminogen activator (tPA), plasminogen activator inhibitor-1 (PAI-1), and D-dimer are significantly higher than those in healthy controls, while α2-antiplasmin levels are lower, indicating a pre-existing degree of functional dysregulation. These alterations are further exacerbated postoperatively, with PAI-1 and D-dimer levels increasing even more relative to preoperative values [17]. Recent research has revealed that the fibrinolytic response after THA is not uniform; rather, two distinct phenotypes exist — "fibrinolytic shutdown" and "non-fibrinolytic shutdown" — which can be identified and stratified using the LY30 parameter on thromboelastography. Patients with the fibrinolytic shutdown phenotype experience significantly less bleeding; however, continuing empirical antifibrinolytic therapy in these patients offers no additional benefit and may subject them to unnecessary drug exposure and potential risks. This finding challenges the traditional paradigm of routine empirical antifibrinolytic therapy after THA and supports the rationale for precision antifibrinolytic strategies [18]. Furthermore, fibrinolytic activation patterns differ significantly between the direct anterior approach (DAA) and the posterolateral approach (PLA) for THA. Postoperative levels of fibrinolysis-related markers — such as the thrombin-antithrombin complex, plasmin-α2-antiplasmin complex, and thrombomodulin — are significantly lower in DAA than in PLA patients, suggesting a relatively lower thrombotic risk after the DAA approach [19]. Maintaining fibrinolytic balance is crucial for perioperative safety in THA patients. Fibrinolytic imbalance can lead to excessive fibrinolysis, increasing occult blood loss and transfusion requirements, or, conversely, to fibrinolytic inhibition, which induces a hypercoagulable state and elevates thrombotic risk. Implementing individualized antifibrinolytic therapy based on fibrinolytic markers such as LY30 significantly reduces

occult blood loss and the decline in hemoglobin in patients with the non-fibrinolytic shutdown phenotype without increasing the incidence of venous thromboembolic events, thus embodying a precision perioperative management strategy centered on maintaining dynamic fibrinolytic balance [18].

This study is the first to integrate network pharmacology with clinical metabolomics to systematically investigate the mechanism of ginsenosides in postoperative antifibrinolysis following THA. Our findings reveal that ginsenosides act in a network-based regulatory mode involving multiple targets (AKT1, PTGS2, JUN), multiple metabolites (arachidonic acid, adenosine), and multiple pathways (complement and coagulation cascades, arachidonic acid metabolism, cGMP-PKG, cAMP), providing a new scientific perspective for the modern application of traditional Chinese medicine.

Network pharmacology analysis indicated that the potential targets of ginsenosides are significantly enriched in the “complement and coagulation cascades” and “platelet activation” pathways, directly pointing to their potential value in regulating the fibrinolytic system. There is complex cross-talk between the complement system and the coagulation-fibrinolysis system [20]. Thrombin not only catalyzes the conversion of fibrinogen to fibrin but also activates complement C5; similarly, plasmin not only degrades fibrin but also activates the complement system [21, 22]. The core targets we identified, such as PLG (plasminogen), F2 (prothrombin), and SERPINE1 (PAI-1), are all key molecules in these two pathways, suggesting that ginsenosides may restore coagulation-fibrinolysis balance by acting on these nodes. Notably, PAI-1, as a key negative regulator of the fibrinolytic system, has become an important target in natural product antifibrinolysis research in recent years. Active ingredients such as salvianolic acid B, baicalein, and astragaloside IV have been shown to significantly downregulate the expression and secretion of PAI-1 in vascular endothelial cells by inhibiting signaling pathways such as NF-κB and ERK/AP-1 [23], providing indirect evidence for an antifibrinolytic effect of ginsenosides via PAI-1 regulation.

Metabolomics analysis revealed significant changes in the plasma metabolic profile of patients after THA. Among these, the arachidonic acid metabolic pathway showed the most prominent changes, manifested by elevated levels of arachidonic acid and its downstream metabolite prostaglandin E2. Arachidonic acid is a precursor for the synthesis of proinflammatory and prothrombotic factors such as prostaglandins and thromboxanes, playing a central role in inflammation and stress states [24, 25]. Its key metabolic enzyme, PTGS2 (COX-2), is also one of the core targets identified by network pharmacology. Molecular docking showed that ginsenoside Rg3 has high binding affinity for PTGS2, suggesting that ginsenosides may reduce the conversion of arachidonic acid to inflammatory prostaglandins by inhibiting PTGS2 activity, thereby alleviating vascular endothelial inflammation and platelet activation and indirectly exerting an antifibrinolytic effect. Du Yuanlin et al. found that dexmedetomidine affects cognitive function by regulating PTGS2 [26], further confirming the importance of this target in perioperative regulation.

Furthermore, integrative analysis also revealed enrichment of the cGMP-PKG and cAMP signaling pathways. These two pathways are critical for regulating vascular tone and platelet function [27]. Nitric

oxide (NO) inhibits platelet aggregation and adhesion by activating the cGMP-PKG pathway. Adenosine, detected by metabolomics, is a potent endogenous platelet inhibitor that increases cAMP levels by activating the adenosine A2A receptor, thereby inhibiting platelet activation [28]. Our PPI network includes ADORA2A (adenosine A2A receptor) and NOS3 (endothelial nitric oxide synthase), suggesting that ginsenosides may regulate adenosine and NO metabolism, activate the cAMP and cGMP-PKG pathways, and thus synergistically inhibit platelet function, mitigating postoperative hypercoagulability and fibrinolytic dysfunction. Recent studies have further revealed that active ingredients of traditional Chinese medicine can also interfere with fibrinolytic resistance and low-shear-stress-induced endothelial inflammation by regulating neutrophil extracellular trap (NET) formation and the Piezo1 mechanosensitive channel [29, 30], offering new research directions for the multi-mechanism regulation of fibrinolysis by ginsenosides.

It is worth noting that JUN (c-Jun), identified through our network pharmacology analysis, is an important component of the AP-1 transcription factor and participates in regulating the expression of various inflammation- and coagulation-related genes. Hypoxanthine in purine metabolism is a marker of oxidative stress and ischemia-reperfusion injury [31]. The changes in adenosine levels detected by metabolomics, together with the JUN target in network pharmacology, collectively suggest that ginsenosides may protect the vascular endothelium through their antioxidant and anti-inflammatory activities, thereby indirectly stabilizing the fibrinolytic system. This is consistent with the previously reported antioxidative stress effects of ginsenoside Rg3 [32, 33].

Strengths and limitations

Network pharmacology relies on existing databases, which may introduce information bias; moreover, the metabolomics sample size is relatively small, and the conclusions require validation in larger cohort studies. Second, this study only performed preliminary validation through molecular docking and lacks in vitro and in vivo functional experiments to verify the phenotypic consequences of overexpressing or knocking down core targets such as AKT1, PTGS2, and PAI-1. In the future, we plan to use Western blotting and RNA interference techniques at the cellular level (e.g., in endothelial cells and platelets) to obtain further direct evidence that ginsenosides exert anti-fibrinolytic effects by regulating specific pathways.

Conclusion

This study is the first to integrate network pharmacology with untargeted metabolomics to systematically elucidate the anti-fibrinolytic mechanism of ginsenosides following total hip arthroplasty (THA). Our findings demonstrate that ginsenosides exert their effects through a multi-target, multi-pathway network, with AKT1, PTGS2, and JUN identified as core targets. Key pathways involved include the complement and coagulation cascades, platelet activation, arachidonic acid metabolism, and the cGMP-PKG/cAMP signaling pathways. Metabolomics further revealed that ginsenosides modulate critical metabolites such as arachidonic acid and adenosine. Molecular docking confirmed strong

binding affinities between key ginsenosides (e.g., Rh7, Rg3, Rh1) and their respective targets (AKT1, JUN, PIK3CA, PTGS2). These results provide a theoretical basis for the perioperative application of ginsenosides as a precision antifibrinolytic strategy in THA patients. Future in vitro and in vivo studies are warranted to validate the functional roles of these targets and pathways.

Abbreviations

THA Total hip arthroplasty

TJA Total joint arthroplasty

PPI Protein-protein interaction

VTE Venous thromboembolism

TBI Traumatic brain injury

MCC Maximal Clique Centrality

OB Oral Bioavailability

DL Drug-Likeness

GO Gene Ontology

KEGG Kyoto Encyclopedia of Genes and Genomes

ASA American Society of Anesthesiologists

BP Biological processes

CC Cellular components

MF Molecular functions

Pre Preoperative

Pos Postoperative

PAI-1 Plasminogen activator inhibitor-1

tPA tissue plasminogen activator

DAA Direct anterior approach

PLA Posterolateral approach

Declarations

Acknowledgments

None.

Author contributions

QXM, YH, and LT contributed to the conception and design of the study. YD and CC contributed to the acquisition and analysis of data. XY wrote the manu script. All authors read and approved the final manuscript.

Funding

This research did not receive any specific grant from funding agencies in the public, commercial, or not-for-profit sectors.

Availability of data and materials

The datasets used and/or analyzed during the current study are available from the corresponding author on reasonable request.

Ethics approval and consent to participate

This study has been approved by the Army Medical Center of PLA; ratification number is 2021(168).

Consent for publication

Not applicable.

Competing interests

The authors declare that they have no competing interests.

References

1. Driesman, A. et al. Total Joint Arthroplasty Is Associated With a Decreased Risk of Traumatic Falls: An Analysis of 499,094 Cases. *J. Am. Acad. Orthop. Surg.* **28** (20), 838–846. https://doi:10.5435/JAAOS-D-19-00541 (2020).
2. Jasper, L. L., Jones, C. A., Mollins, J., Pohar, S. L. & Beaupre, L. A. Risk factors for revision of total knee arthroplasty: a scoping review. *BMC Musculoskelet. Disord*. **17**, 182. https://doi:10.1186/s12891-016-1025-8 (2016).
3. Kurtz, S., Ong, K., Lau, E., Mowat, F. & Halpern, M. Projections of primary and revision hip and knee arthroplasty in the United States from 2005 to 2030. *J. Bone Joint Surg. Am.* **89** (4), 780–785.

https://doi:10.2106/JBJS.F.00222 (2007).

4. Wang, C. et al. Dynamic changes of coagulation and fibrinolytic biomarkers in peri operaive arthroplasty patients. *J. Pak Med. Assoc.* **70** (12(B)), 2422–2426. https://doi:10.47391/JPMA.748 (2020).
5. Ezaki, M. et al. Plasma Soluble Fibrin Is Useful for the Diagnosis of Thrombotic Diseases. *J. Clin. Med.* **12** (7), 2597. https://doi:10.3390/jcm12072597 (2023).
6. Samuels, J. M. et al. Obesity is associated with postinjury hypercoagulability. *J. Trauma. Acute Care Surg.* **87** (4), 876–882. https://doi:10.1097/TA.0000000000002414 (2019).
7. Fu, X. et al. Comparison of robotic-assisted total knee arthroplasty: an updated systematic review and meta-analysis. *J. Robot Surg.* **18** (1), 292. https://doi:10.1007/s11701-024-02045-y (2024).
8. Tao, X. et al. Ginsenoside Rg3 Mitigates LPS-Induced Injury in Human Bronchial Epithelial Cells by Restoring Autophagic Flux and Inhibiting the TLR4/NF-κB-Mediated Inflammatory Response. *J. Inflamm. Res.* **19**, 555053. https://doi:10.2147/JIR.S555053 (2026).
9. Zhu, H. et al. Pharmacological activation of SIRT1-AMPK by ginsenoside Rb1: a novel therapeutic strategy for pressure injury *via* dual suppression of ferroptosis and inflammation. *Front. Pharmacol.* **16**, 1683479. https://doi:10.3389/fphar.2025.1683479 (2026).
10. Wang, J. et al. Screening of anti-platelet aggregation agents from Panax notoginseng using human platelet extraction and HPLC-DAD-ESI-MS/MS. *J. Sep. Sci.* **31** (6–7), 1173–1180. https://doi:10.1002/jssc.200700507 (2008).
11. Lee, Y. Y. et al. Ginsenoside Rg3-enriched red ginseng extract mitigates sepsis by inhibiting platelet-leukocyte aggregates and regulates thrombo-inflammatory pathways. *J. Ginseng Res.* **50** (1), 100909. https://doi:10.1016/j.jgr.2025.10.006. (2026). Epub 2025 Oct 26.
12. Li, X. et al. Integrated network pharmacology and metabolomics to dissect the combination mechanisms of Bupleurum chinense DC-Paeonia lactiflora Pall herb pair for treating depression. *J. Ethnopharmacol.* **264**, 113281. https://doi:10.1016/j.jep.2020.113281. (2021). Epub 2020 Aug 15.
13. Li, T. et al. Integrated metabolomics and network pharmacology to reveal the mechanisms of hydroxysafflor yellow A against acute traumatic brain injury. *Comput. Struct. Biotechnol. J.* **19**, 1002–1013. https://doi:10.1016/j.csbj.2021.01.033 (2021).
14. Hui, R. et al. Parthenolide inhibits methamphetamine-induced depressive-like behavior by targeting ADORA2A. *Phytomedicine* **154**, 158030. https://doi:10.1016/j.phymed.2026.158030. (2026). Epub 2026 Mar 1.
15. Zhao, X., Xiu, J., Yang, H., Han, W. & Jin, Y. Network Pharmacology and Bioinformatics Study of Six Medicinal Food Homologous Plants Against Colorectal Cancer. *Int. J. Mol. Sci.* **26** (3), 930. https://doi:10.3390/ijms26030930 (2025).
16. Cho, J. H. et al. A novel black ginseng processing method for optimizing rare ginsenosides with bioactivity and sustainability. *J. Ginseng Res.* **50** (2), 100933. https://doi:10.1016/j.jgr.2025.100933. (2026). Epub 2025 Dec 18.

17. Guler, N. et al. Fibrinolytic Dysregulation in Total Joint Arthroplasty Patients: Potential Clinical Implications. *Clin. Appl. Thromb. Hemost.* **22** (4), 372–376. https://doi:10.1177/1076029615597060. (2016). Epub 2015 Jul 22.
18. Luo, X. et al. Revolutionizing Antifibrinolytic Therapy: Personalized Strategies for Total Hip Arthroplasty Patients Who Have Divergent Fibrinolytic Responses. *J. Arthroplasty 2025 Aug* **20**: S0883-5403(25)01037-X. https://doi:10.1016/j.arth.2025.08.029. Epub ahead of print.
19. Liu, R. et al. Comparative efficacy of direct anterior approach versus conventional surgical approaches in total hip arthroplasty: a systematic review and meta-analysis of randomized clinical trials. *J. Orthop. Surg. Res.* **20** (1), 837. https://doi:10.1186/s13018-025-06227-8 (2025).
20. Martin, M. et al. Emerging role of nucleic acid aptamers in sepsis-induced coagulopathy: Future perspectives in diagnostics and therapeutics. *Ann. Intensive Care*. **16**, 100014. https://doi:10.1016/j.aicoj.2025.100014 (2026).
21. Amara, U. et al. Molecular intercommunication between the complement and coagulation systems. *J. Immunol.* **185** (9), 5628–5636. https://doi:10.4049/jimmunol.0903678. (2010). Epub 2010 Sep 24.
22. Mollnes, T. E., Storm, B. S., Brekke, O. L., Nilsson, P. H. & Lambris, J. D. Application of the C3 inhibitor compstatin in a human whole blood model designed for complement research – 20 years of experience and future perspectives. *Semin Immunol.* **59**, 101604. https://doi:10.1016/j.smim.2022.101604. (2022). Epub 2022 May 13.
23. Gong, P. Y. et al. Reverse tracing anti-thrombotic active ingredients from dried Rehmannia Radix based on multidimensional spectrum-effect relationship analysis of steaming and drying for nine cycles. *J. Ethnopharmacol.* **276**, 114177. https://doi:10.1016/j.jep.2021.114177. (2021). Epub 2021 May 1.
24. Huang, Z. et al. Mulberry (Morus alba l.) leaf improves arachidonic acid metabolism disorder in chronic obstructive pulmonary disease. *Phytomedicine* **148**, 157392. https://doi:10.1016/j.phymed.2025.157392. (2025). Epub 2025 Oct 15.
25. Szczuko, M. et al. Lipoxin (LTX A4 5S, 6R, 15R) levels drastically decrease after 5 years of hemodialysis treatment. *J. Physiol. Pharmacol.* **71** (3). https://doi:10.26402/jpp.2020.3.10. (2020). Epub 2020 Oct 15.
26. Du, Y. et al. Integrated analysis of metabolomics combined and net-work pharmacology reveals the effects of dexmedetomidine on early postoperative cognitive dysfunction in elderly patients: randomized controlled trial. *BMC Anesthesiol*. **26** (1), 33. https://doi:10.1186/s12871-025-03379-2 (2025).
27. Smolenski, A. Novel roles of cAMP/cGMP-dependent signaling in platelets. J Thromb Haemost. ;10(2):167 – 76. https://doi: (2012). 10.1111/j.1538-7836.2011.04576. x.
28. Johnston-Cox, H. A. & Ravid, K. Adenosine and blood platelets. *Purinergic Signal.* **7** (3), 357–365. 10.1007/s11302-011-9220-4. (2011). https:// Epub 2011 Feb 8.
29. Chala, D. et al. Immunomodulatory and antibacterial effect of red wine concentrate rich in a natural complex of polyphenols under diabetes mellitus. *Biomed. Pharmacother*. **170**, 116023.

https://doi:10.1016/j.biopha.2023.116023. (2024). Epub 2023 Dec 16.

30. Lu, Y. et al. Efficacy and mechanism study of Baichanting compound, a combination of Acanthopanax senticosus (Rupr. and Maxim.) Harms, Paeonia lactiflora Pall and Uncaria rhynchophylla (Miq.) Miq. ex Havil, on Parkinson's disease based on metagenomics and metabolomics. J Ethnopharmacol. ;319(Pt 1):117182. (2024). https://doi:10.1016/j.jep.2023.117182. Epub 2023 Sep 13.
31. Glantzounis, G. K., Tsimoyiannis, E. C., Kappas, A. M. & Galaris, D. A. Uric acid and oxidative stress. *Curr. Pharm. Des.* **11** (32), 4145–4151. https://doi:10.2174/138161205774913255 (2005).
32. Huang, Y. et al. Anti-skin aging effects of black ginseng extracts through regulating inflammatory factors and the CLOCK-ERK pathway in mice. *J. Ginseng Res.* **50** (2), 100926. https://doi:10.1016/j.jgr.2025.11.014 (2026). Epub 2025 Dec 2. P.
33. Wang, Y. et al. Ginsenoside RG3 and cantharidin synergistically suppress the progression of hepatocellular carcinoma via targeting the PRMT1-SREBF1 axis-mediated lipid metabolism. *J. Transl Med.* **24** (1), 78. https://doi:10.1186/s12967-025-07550-8 (2026).

Tables

Tables 1 and 2 are available in the Supplementary Files section.

Figures

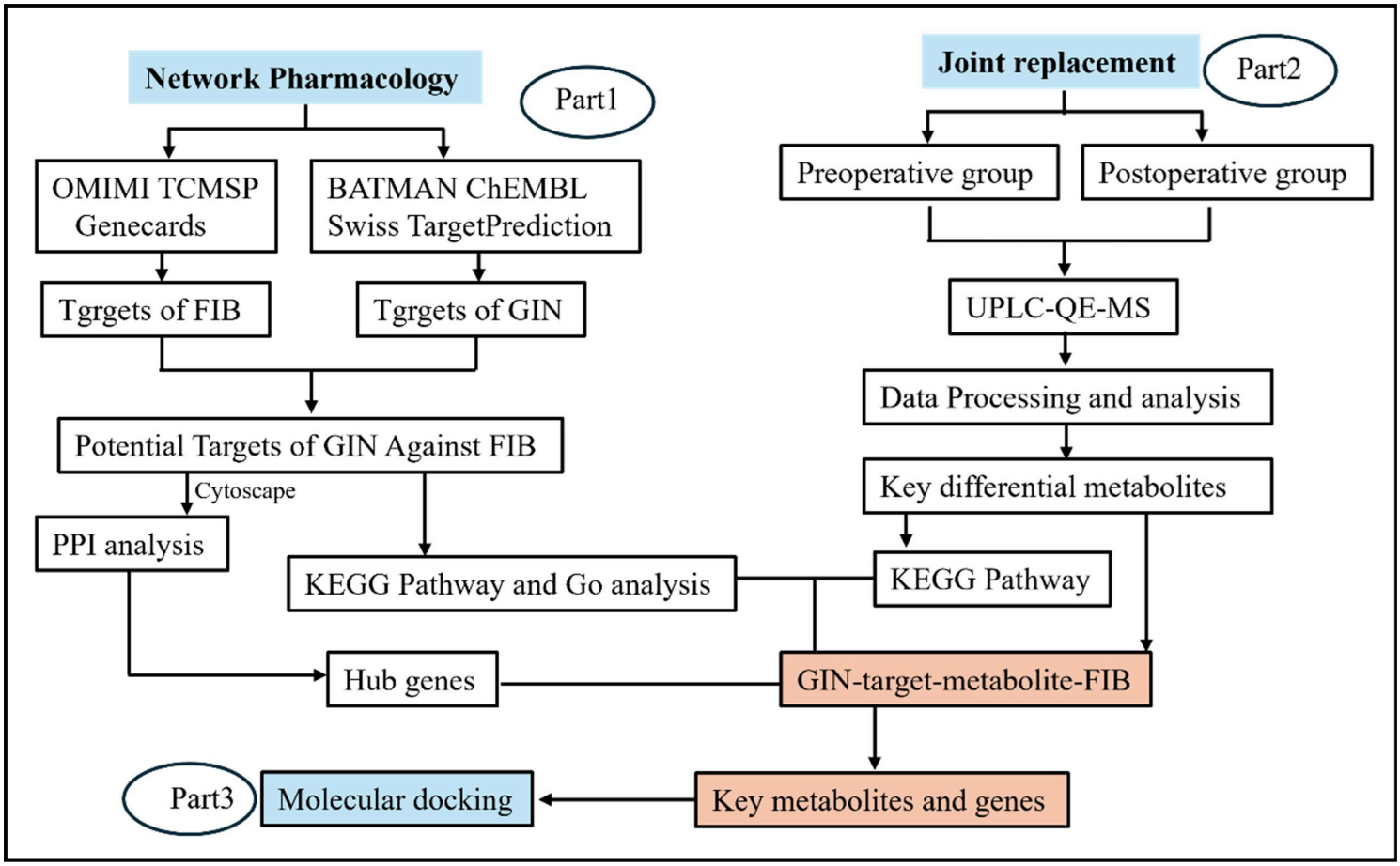


Figure 1

Workflow diagram. We employed network pharmacology to analyze the effects of active ginsenoside components on fibrinolysis and identify key target genes. To further investigate the impact of ginsenosides on anti-fibrinolysis in arthroplasty, we used metabolomics to analyze changes in differential metabolites between preoperative and postoperative states and performed pathway enrichment. Finally, we integrated the enriched pathways from metabolomics and network pharmacology to construct a comprehensive drug-gene-metabolite-disease network.

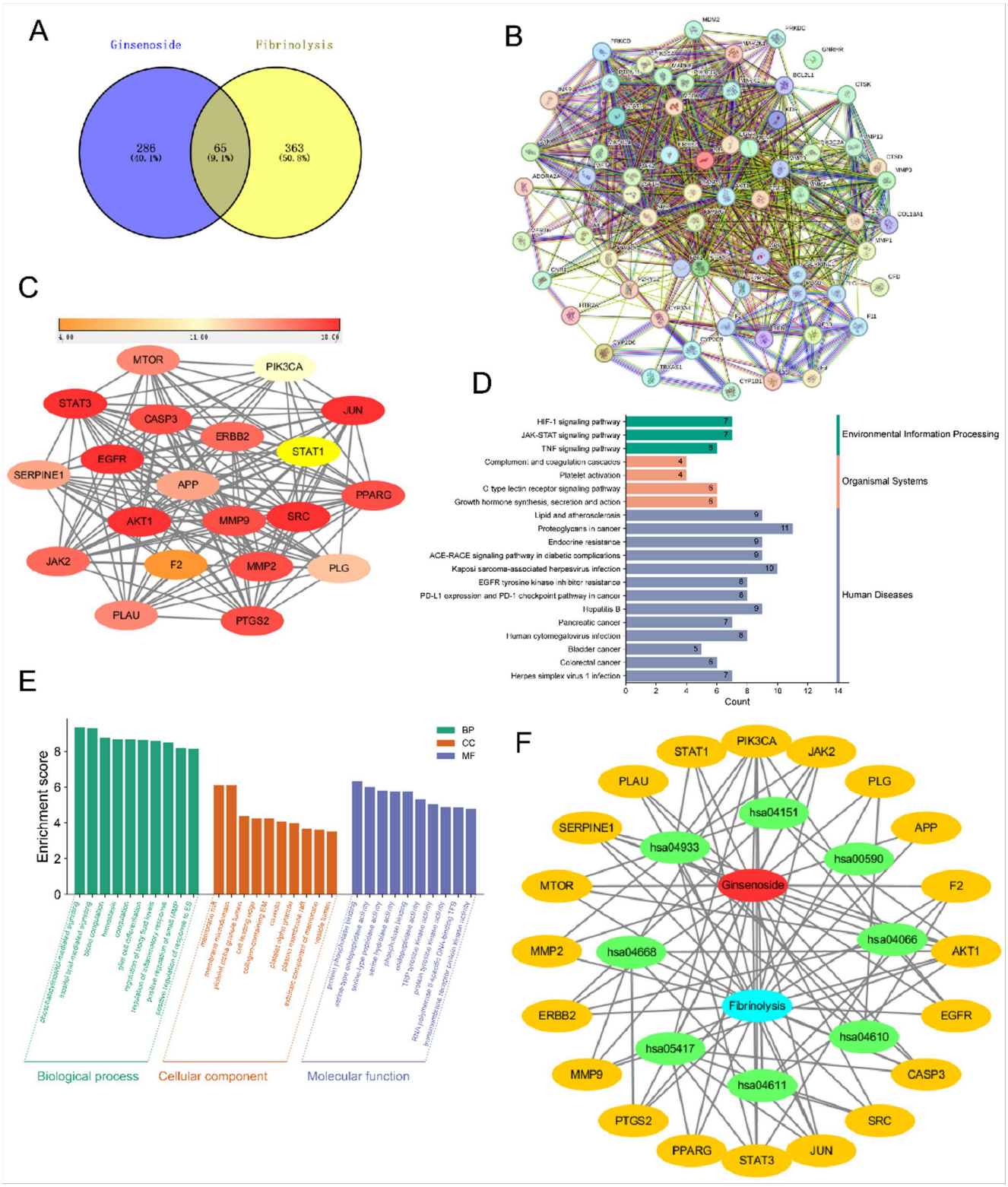


Figure 2

Network pharmacology analysis of the effect of ginsenosides on fibrinolysis. A. Venn diagram showing ginsenoside-related and fibrinolysis-related target genes. B. Protein-protein interaction (PPI) network analysis. C. Core target gene network. D. KEGG pathway enrichment analysis. E. GO enrichment analysis. F. Component-target-pathway-disease network.

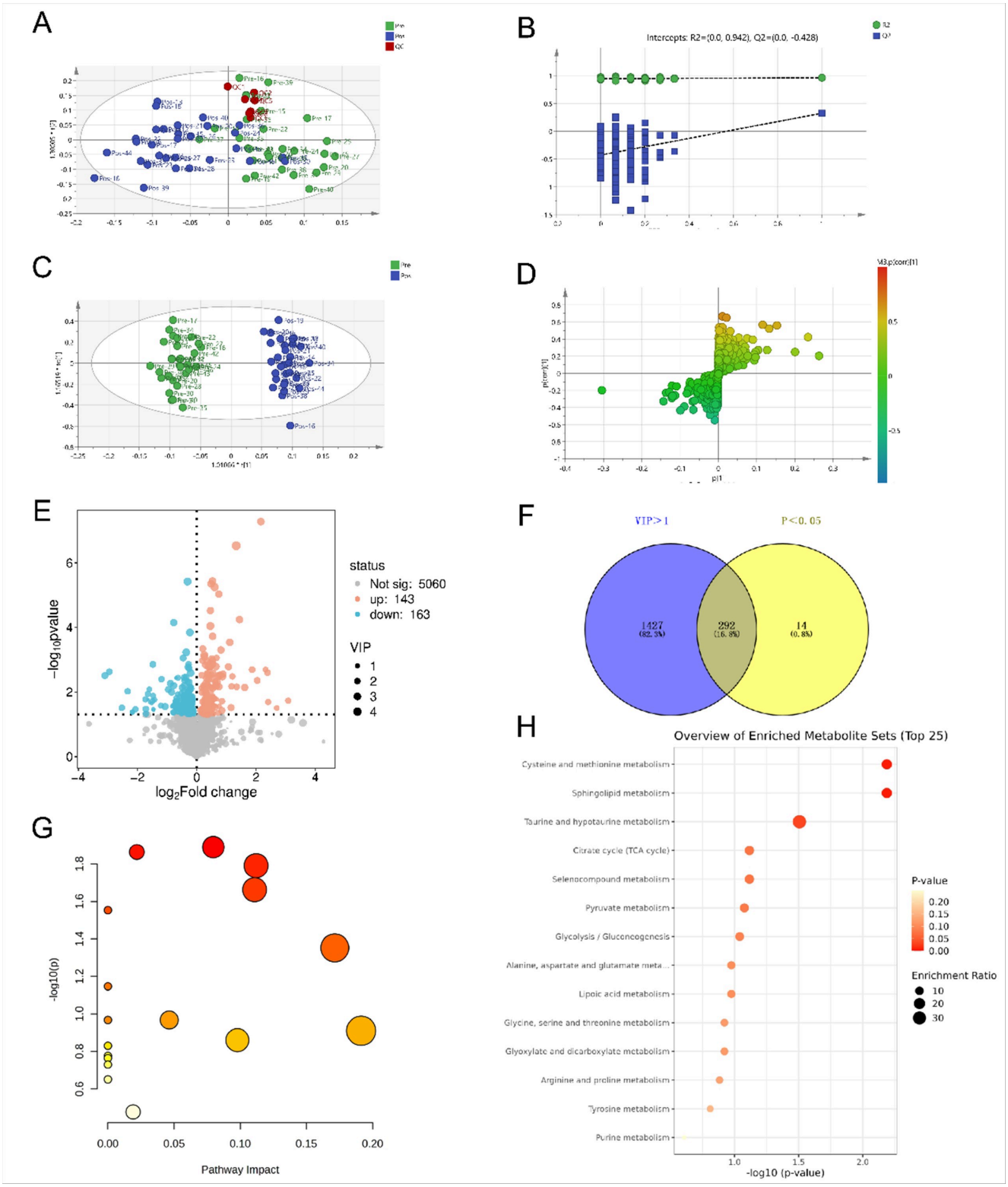
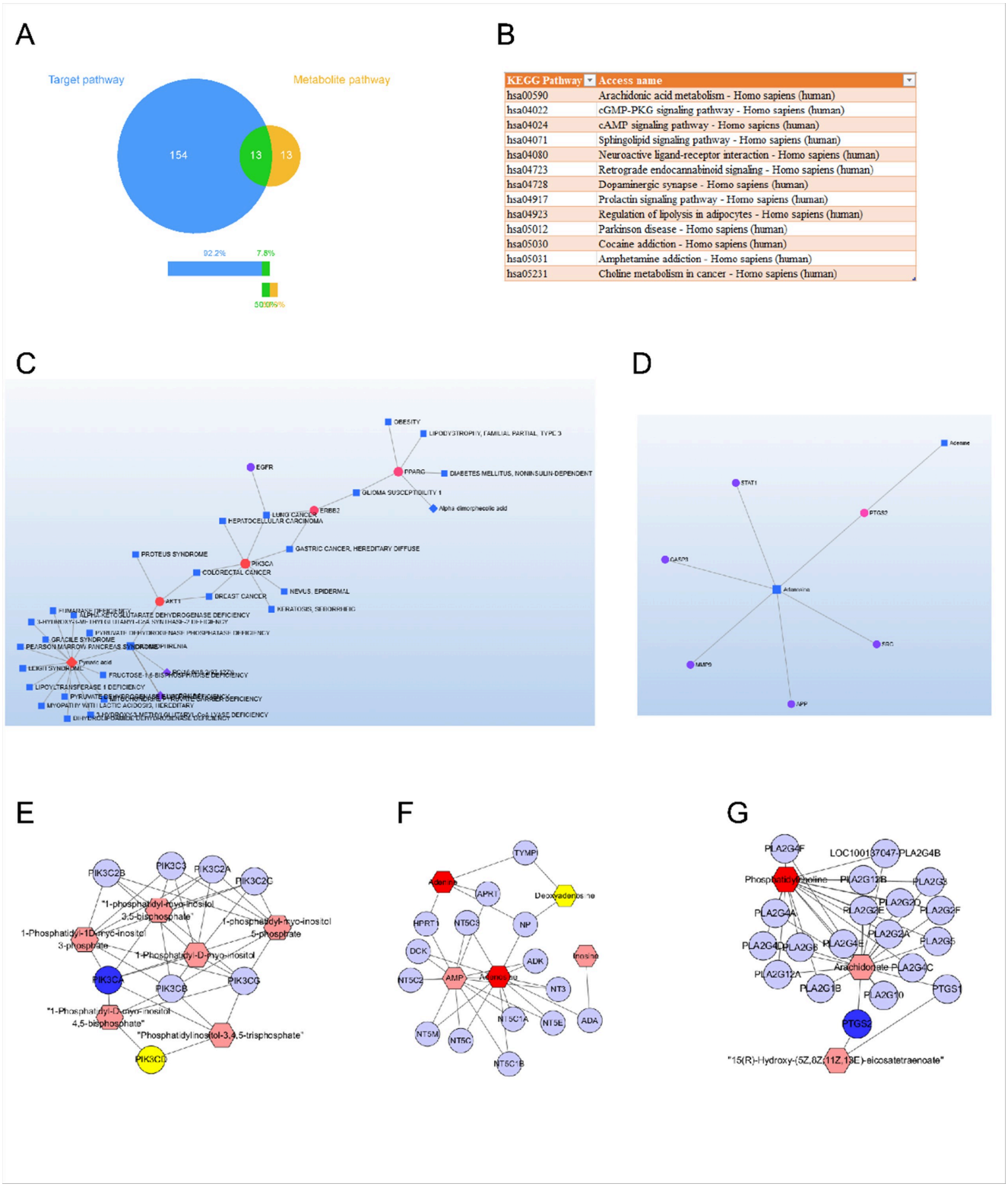


Figure 3

Metabolomics analysis results of blood samples from arthroplasty patients preoperatively and postoperatively. A. Score scatter plot of the PCA model for group Pre vs. group Pos in positive and negative ion modes. Green indicates the Pre group, and blue indicates the Pos group. B. PLS-DA model validation plot. C. OPLS-DA score plot. D. S-plot of OPLS-DA. E. Volcano plot analysis. F. Screening of

differential metabolites between preoperative and postoperative states. G-H. Enriched pathway analysis of differential metabolites.

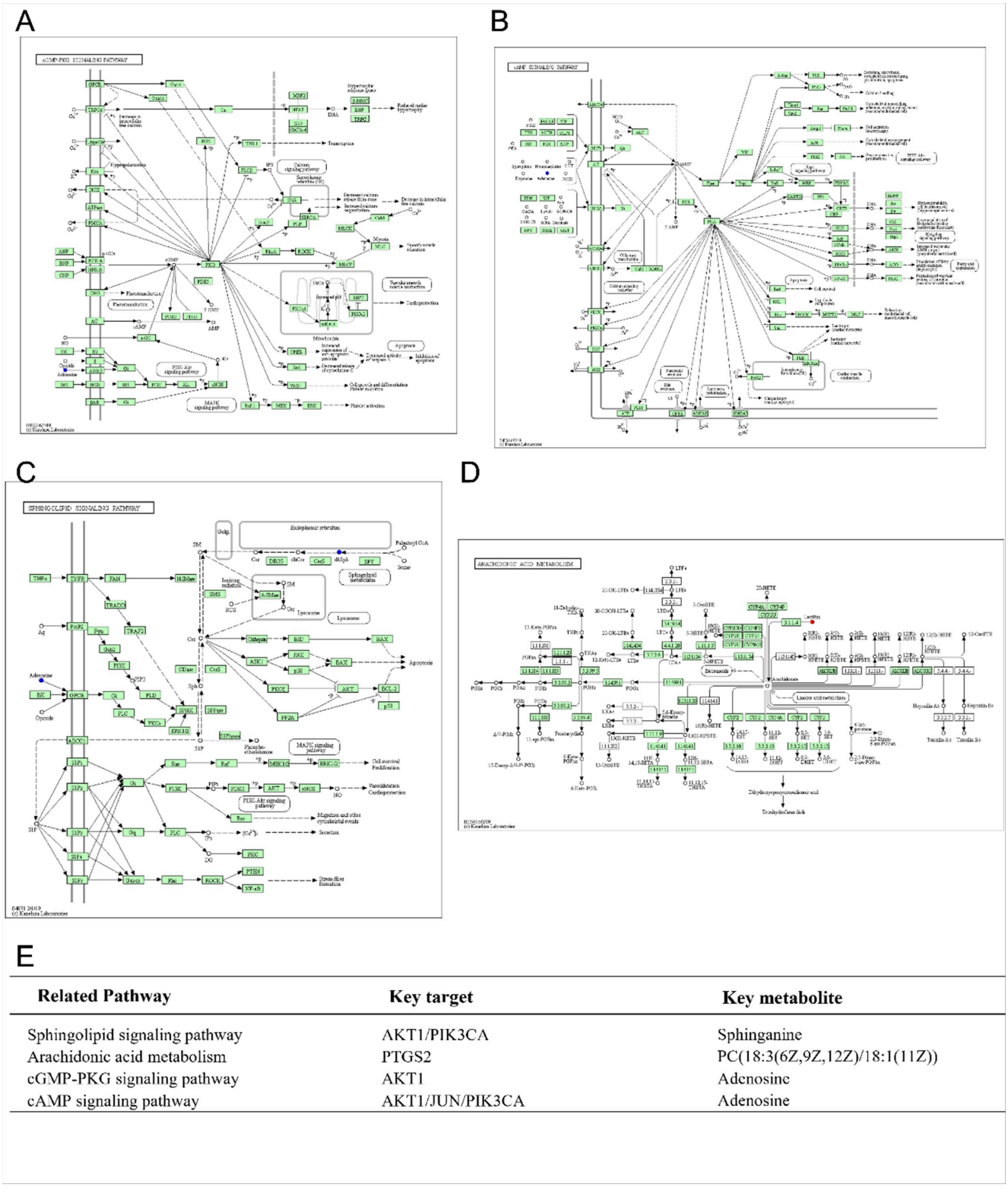


KEGG Pathway	Access name
hsa00590	Arachidonic acid metabolism - Homo sapiens (human)
hsa04022	cGMP-PKG signaling pathway - Homo sapiens (human)
hsa04024	cAMP signaling pathway - Homo sapiens (human)
hsa04071	Sphingolipid signaling pathway - Homo sapiens (human)
hsa04080	Neuroactive ligand-receptor interaction - Homo sapiens (human)
hsa04723	Retrograde endocannabinoid signaling - Homo sapiens (human)
hsa04728	Dopaminergic synapse - Homo sapiens (human)
hsa04917	Prolactin signaling pathway - Homo sapiens (human)
hsa04923	Regulation of lipolysis in adipocytes - Homo sapiens (human)
hsa05012	Parkinson disease - Homo sapiens (human)
hsa05030	Cocaine addiction - Homo sapiens (human)
hsa05031	Amphetamine addiction - Homo sapiens (human)
hsa05231	Choline metabolism in cancer - Homo sapiens (human)

Figure 4

Integrative analysis using network pharmacology and metabolomics. A. Intersection pathways between ginsenoside-related fibrinolytic pathways and metabolic pathways. B. Information on common

pathways. C. Metabolite-gene-disease association network. D. Metabolite-gene association network. E-G. Key metabolites and targets in the composite reaction-enzyme-gene network. Red hexagons, green circular rectangles, and purple circles represent active compounds, proteins, and genes, respectively.



Related Pathway	Key target	Key metabolite
Sphingolipid signaling pathway	AKT1/PIK3CA	Sphinganine
Arachidonic acid metabolism	PTGS2	PC(18:3(6Z,9Z,12Z)/18:1(11Z))
cGMP-PKG signaling pathway	AKT1	Adenosine
cAMP signaling pathway	AKT1/JUN/PIK3CA	Adenosine

Figure 5

Illustration of metabolic pathways. A. cGMP-PKG signaling pathway. B. cAMP signaling pathway. C. Sphingolipid signaling pathway. D. Arachidonic acid metabolism pathway. E. Information on key targets, metabolites, and pathways.

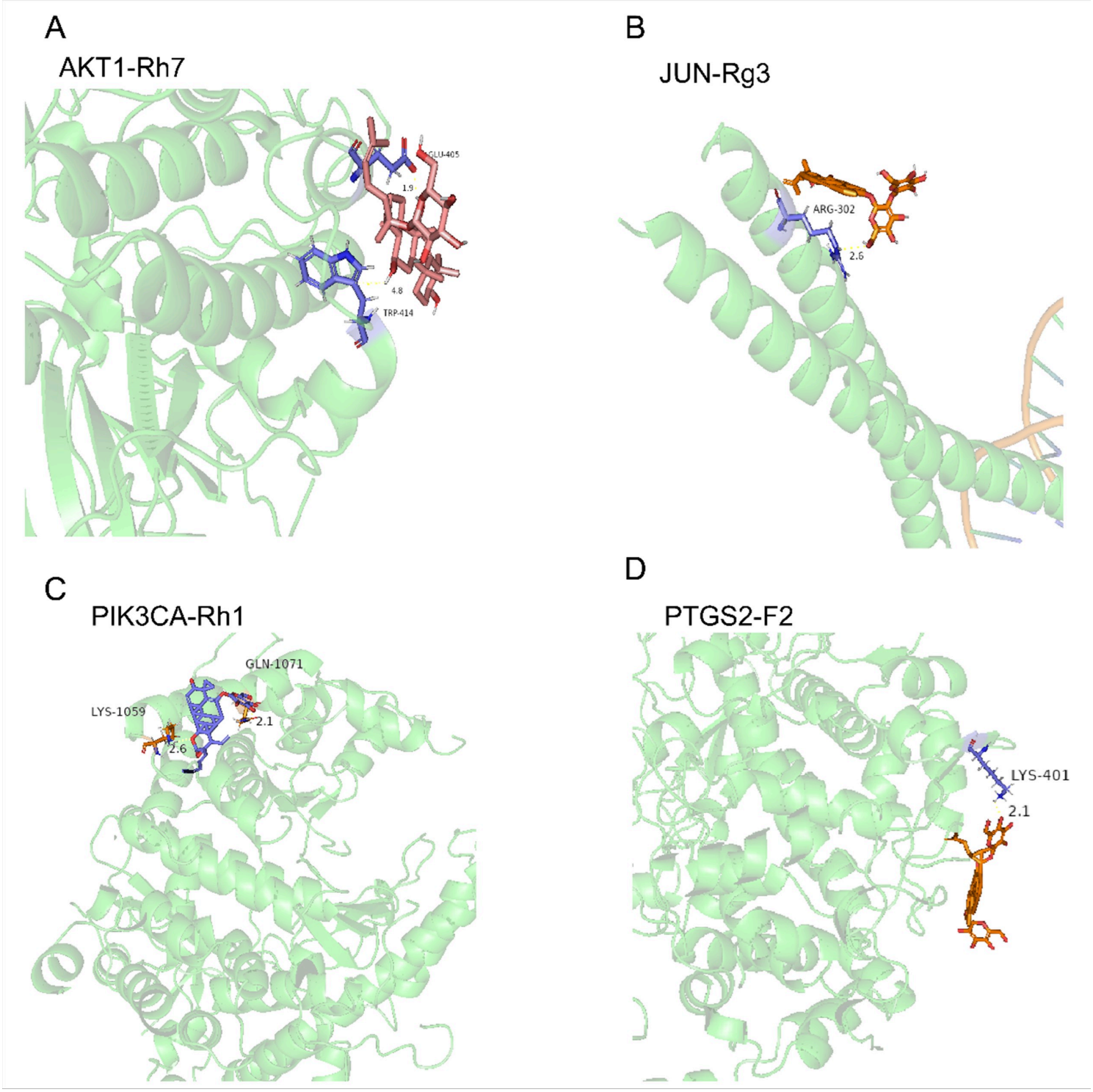


Figure 6

3D interaction diagrams of ginsenosides and their key targets.

Supplementary Files

This is a list of supplementary files associated with this preprint. Click to download.

- Table1.docx
- Table2.docx